Tuning Activity and Selectivity during Alkyne Activation by Gold(I)/Platinum(0) Frustrated Lewis Pairs

Nereida Hidalgo, Juan José Moreno, Marina Pérez-Jiménez, Celia Maya, Joaquín López-Serrano*, Jesús Campos*

Instituto de Investigaciones Químicas (IIQ), Departamento de Química Inorgánica and Centro de Innovación en Química Avanzada (ORFEO-CINQA). Universidad de Sevilla and Consejo Superior de Investigaciones Científicas (CSIC). Avenida Américo Vespucio 49, 41092 Sevilla (Spain).

*jesus.campos@iiq.csic.es; * joaquin.lopez@iiq.csic.es

SUPPORTING INFORMATION

1. Additional computational details

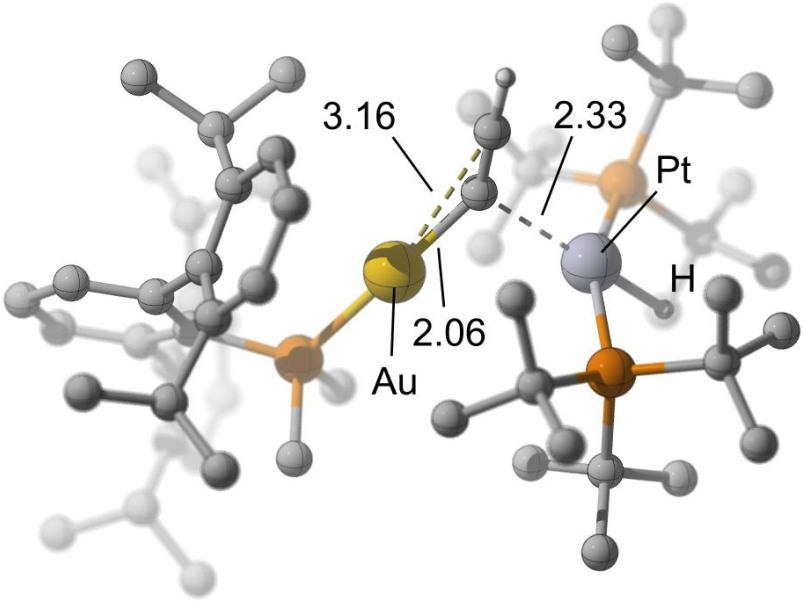

Figure S1. Optimized geometry for σ,π-isomerization of the bridging μ-C≡CH, $TS_{C\rightarrow 4a}$, to yield acetylide **3b**.

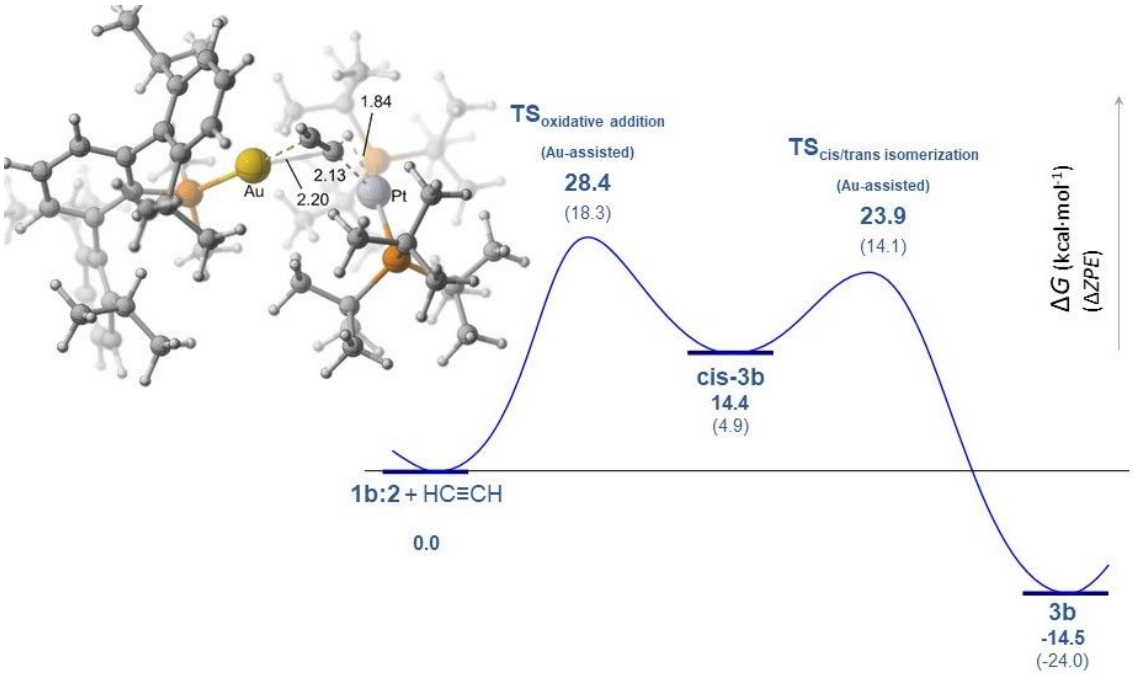

Figure S2. Energy profile for alternative orthogonal mechanism involving the initial oxidative addition of acetylene over **2**, followed by cis-trans isomerization.

Regarding the profile of Figure S2, a parallel mechanism was calculated without the participation of the Au fragment. Energy barriers for oxidative addition and isomerization are higher at $\Delta G^{\ddagger}$ = 30.0 and 34.7 kcal·mol^{-1} respectively.

2. X-Ray Structural Characterization of new compounds

Single crystals of suitable size of each compound were selected and covered with FOMBLIN oil and mounted on a glass fiber. Data collections have been performed on two X-ray diffractometers:

- a Bruker-AXSX8Kappa diffractometer equipped with an Apex-II CCD area detector, using a graphite monochromator Ag Kα1 (λ=0.56086 Å) or Cu Kα1 (λ=0.56086 Å) and a Bruker Cryo-Flex low-temperature device (used with **3a**).

- a Bruker SMART APEX II CCD area detector on a D8 goniometer, using graphite-monochromated and 0.5 mm-Monocap-collimated Mo-K_α radiation (λ=0.71073 Å) (used with **4c**).

- a Bruker Bruker D8 Quest APEX-III CCD area detector PhotonIII using monochromatic radiation λ (Mo Kα1) = 0.71073 Å by a IμS 3.0 microfocus X-ray source (used with **10**, **11b, 12a** and **13b**).

Data collections were processed with APEX-W2D-NT (Bruker, 2004), cell refinement and data reduction with SAINT-Plus (Bruker, 2004) and the absorption was corrected by multiscan method applied by SADABS.[1] The space-group assignment was based upon systematic absences, E statistics, and successful refinement of the structure. The structure was solved by direct methods and expanded through successive difference Fourier maps, F^2 (SHELXTL).[2] In the last cycles of refinement, ordered non-hydrogen atoms were refined anisotropically whereas disordered partial occupancy non-hydrogen atoms in structure **4c** were refined isotropically. Hydrogen atoms connected to carbon atoms were included in idealized positions, and a riding model was used for their refinement.

In structure **3a**, DFIX and SADI commands have been used to restrain the hydride bonded to platinum. In structure **4c**, there are two molecules in the asymmetric unit and in one of them, the therphenyl group was disordered over two sites the occupancies of which were constrained to sum to 1.0. This disorder was modelled using the following restrains in the aromatic rings: SADI (0.01), FLAT, DELU and SIMU. In structure **12a**, DFIX and SADI commands have been used to restrain tri-tert-butylphosphine ligands and bistriflimide anions. In structure **11b**, SADI commands have been used to restrain bistriflimide anions. Additionally, in both structures, **4c** and **11b**, refinement showed residual electron density due to heavily disordered solvent molecules, and even a counterion in case of **4c**, which could not be modelled. Therefore the option SQUEEZE of the program package PLATON[3] was used to create an hkl file taking into account the residual electron density in the void areas.

A summary of all crystallographic data and refinement parameters for each compound is provided in Tables S1 and S2. Atomic coordinates, anisotropic displacement parameters and bond lengths and angles can be found in the cif files which have been deposited in the Cambridge Crystallographic Data Centre with no. 1965525, 1965526 and 1986501-1986504. These data can be obtained free of charge from The Cambridge Crystallographic Data Centre via www.ccdc.cam.ac.uk/data_request/cif.

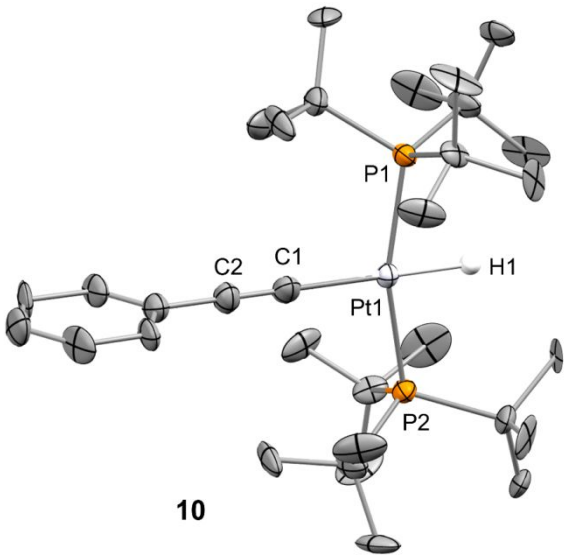

Figure S3. ORTEP diagram of compound **10**; for the sake of clarity most hydrogen atoms are excluded. Thermal ellipsoids are set at 50 % probability.

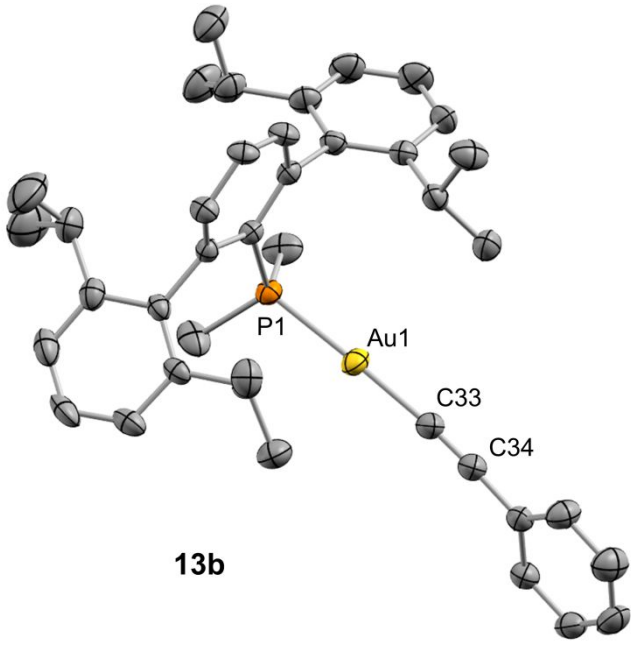

Figure S4. ORTEP diagram of compound **13b**; for the sake of clarity hydrogen atoms are excluded. Thermal ellipsoids are set at 50 % probability.

Table S1. Crystal data and structure refinement for compounds **3a, 4c** and **10**.

	3a	**4c**	**10**
formula	$C_{52}H_{83}AuF_6NO_4P_3PtS_2$	$C_{144}H_{200}Au_2F_7NO_6P_6Pt_2S_7$	$C_{32}H_{59}P_2Pt$
fw	1449.28	3368.39	700.82
cryst.size, mm	0.32 x 0.15 x 0.10	0.24 x 0.21 x 0.18	0.26 x 0.21 x 0.17
crystal system	Monoclinic	Triclinic	Orthorhombic
space group	$P2_1/c$	P-1	$C222_1$
a, Å	23.6949(14)	16.5214(4)	11.4795(4)
b, Å	12.2437(7)	17.1816(4)	25.8563(9)
c, Å	20.0699(10)	27.9487(8)	11.0959(3)
α, deg	90	90.227(1)	90
β, deg	92.523(2)	96.543(1)	90
γ, deg	90	114.489(1)	90
V, Å^3	5816.9(6)	7161.4(3)	3293.46(19)
T, K	173	173	193
Z	4	2	4
ρ_{calc}, g cm^{-3}	1.655	1.562	1.413
μ, mm^{-1} (MoKα)	2.795	4.221	4.38
F(000)	2888	3396	1436
absorption corrections	multi-scan, 0.57-0.75	multi-scan, 0.75-0.41	multi-scan, 0.48-0.75
θ range, deg	1.48 to 23.71	0.73 to 28.35.	1.94 – 28.30
no. of rflns measd	206308	151547	33652
R_{int}	0.074	0.046	0.060
no. of rflns unique	17848	35284	4094
no. of params / restraints	662 / 2	1406 / 178	238 / 2
R_1 ($I > 2\sigma(I)$) [a]	0.044	0.077	0.025
R_1 (all data)	0.069	0.113	0.031
wR_2 ($I > 2\sigma(I)$)	0.125	0.218	0.079
wR_2 (all data)	0.146	0.236	0.089
Diff.Fourier.peaks min/max, eÅ^{-3}	-3.013 / 4.159	-4.733 / 7.214	-0.925 / 3.030
CCDC number	1965525	1965523	1986502

Table S2. Crystal data and structure refinement for compounds **11b**, **12a** and **13b**.

	11b	**12a**	**13b**
formula	$C_{81}H_{99}Au_2F_6NO_4P_2S_2$	$C_{58}H_{86}AuF_6N_2O_4P_3PtS_2$	$C_{40}H_{48}AuP$
fw	1784.60	1538.37	756.72
cryst.size, mm	0.31 x 0.23 x 0.16	0.28 x 0.22 x 0.17	0.45 × 0.37 × 0.32
crystal system	Monoclinic	Triclinic	Monoclinic
space group	$P2_1/c$	*P-1*	$P2_1/c$
a, Å	13.3472(6)	11.2581(6)	13.6424 (11),
b, Å	34.7044(15)	12.8768(7)	21.0315 (15),
c, Å	20.7071(8)	22.6311(10)	12.4138 (8)
α, deg	90	94.192(2)	90
β, deg	107.628(2)	97.562(2)	98.189 (3)
γ, deg	90	100.169(2)	90
V, Å^3	9141.3(7)	3185.5(3)	3525.5 (4)
T, K	193	193	193
Z	4	2	4
ρ_{calc}, g cm^{-3}	1.297	1.604	1.426
μ, mm^{-1} (MoKα)	3.34	4.70	4.24
F(000)	3592	1536	1528
absorption corrections	multi-scan, 0.57-0.75	multi-scan, 0.58-0.74	multi-scan, 0.47-0.75
θ range, deg	1.99 – 25.71	1.93 – 25.68	2.3 – 28.3
no. of rflns measd	75414	35926	63370
R_{int}	0.083	0.050	0.062
no. of rflns unique	17341	12067	8741
no. of params / restraints	904 / 38	808 / 111	389 / 0
R_1 ($I > 2\sigma(I)$) [a]	0.066	0.047	0.035
R_1 (all data)	0.096	0.061	0.056
wR_2 ($I > 2\sigma(I)$)	0.182	0.139	0.099
wR_2 (all data)	0.199	0.149	0.129
Diff.Fourier.peaks min/max, eÅ^{-3}	-2.100 / 2.936	-1.644 / 1.837	-1.84 / 1.70
CCDC number	1986504	1986503	1986501

3. NMR spectra of new compounds.

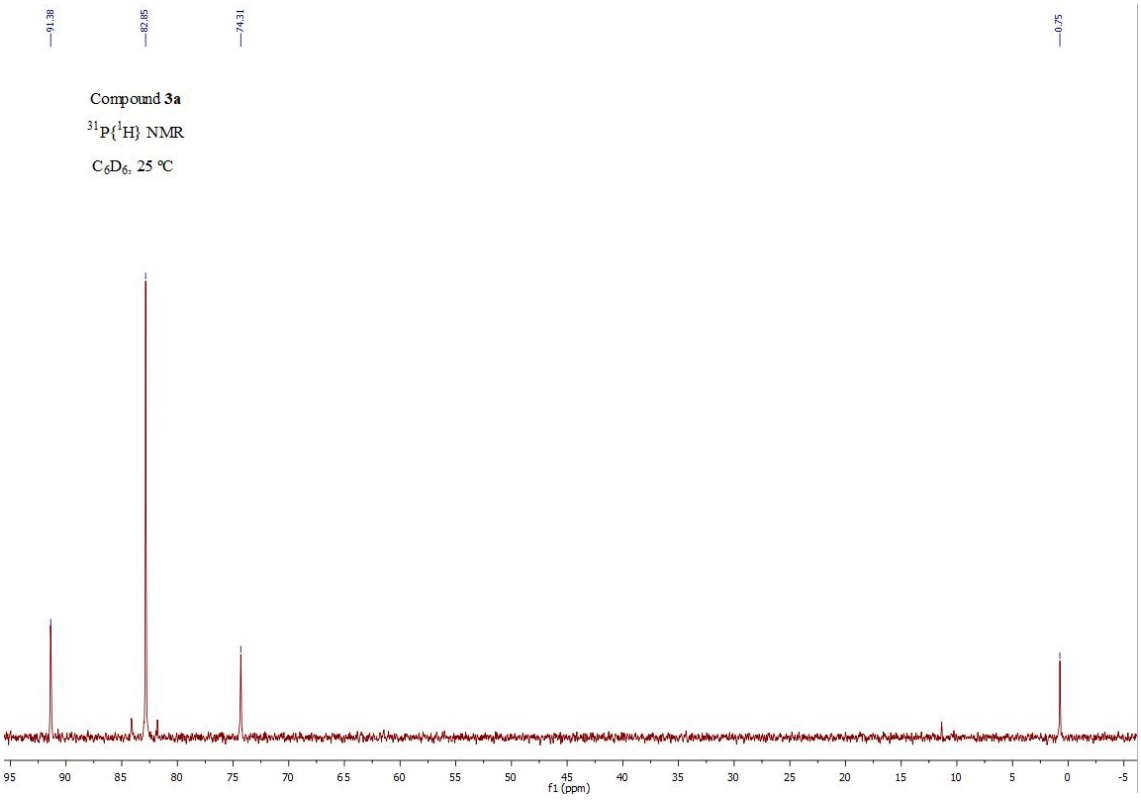

Figure S5. $^{31}P\{^{1}H\}$ NMR spectrum of compound **3a**.

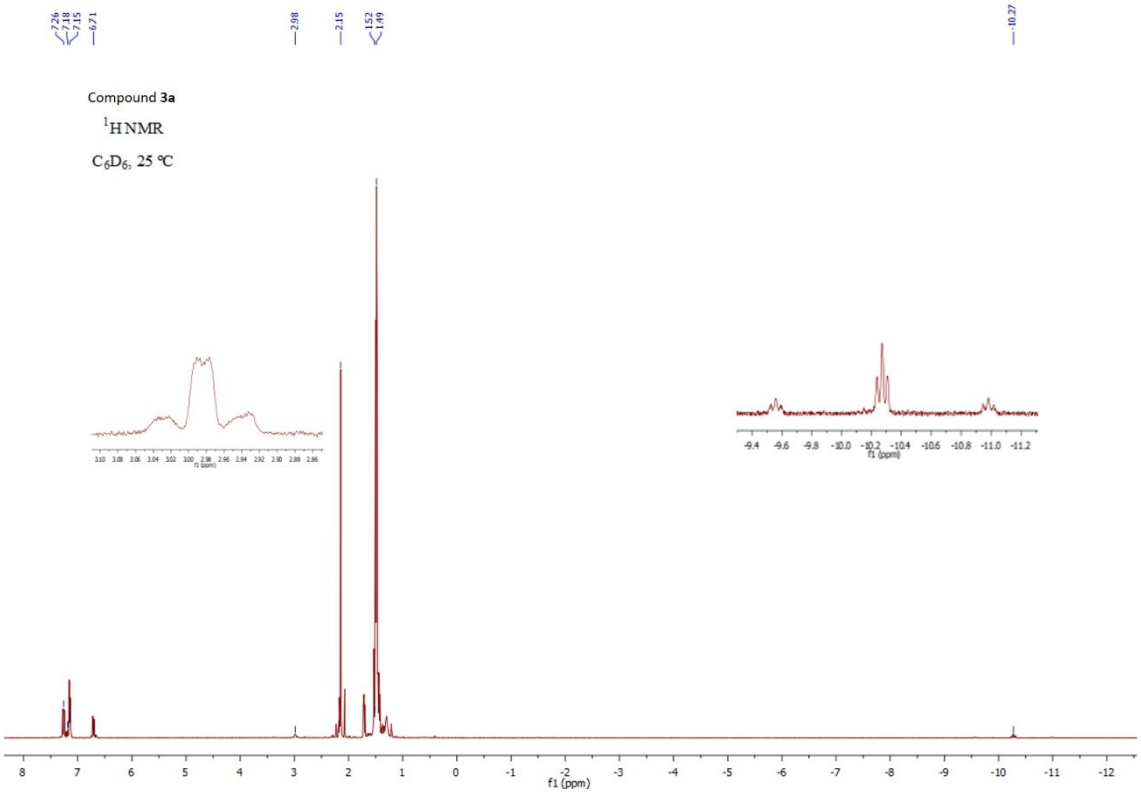

Figure S6. ^{1}H NMR spectrum of compound **3a**.

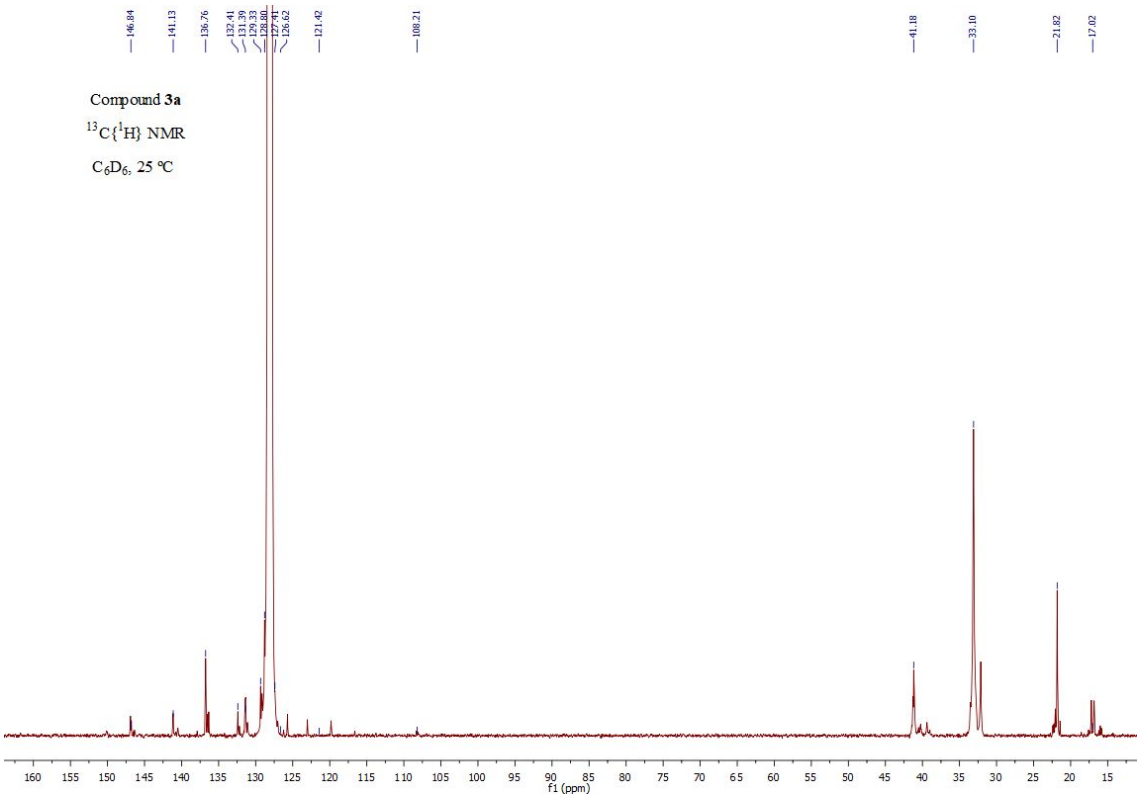

Figure S7. $^{13}C\{^{1}H\}$ NMR spectrum of compound **3a**.

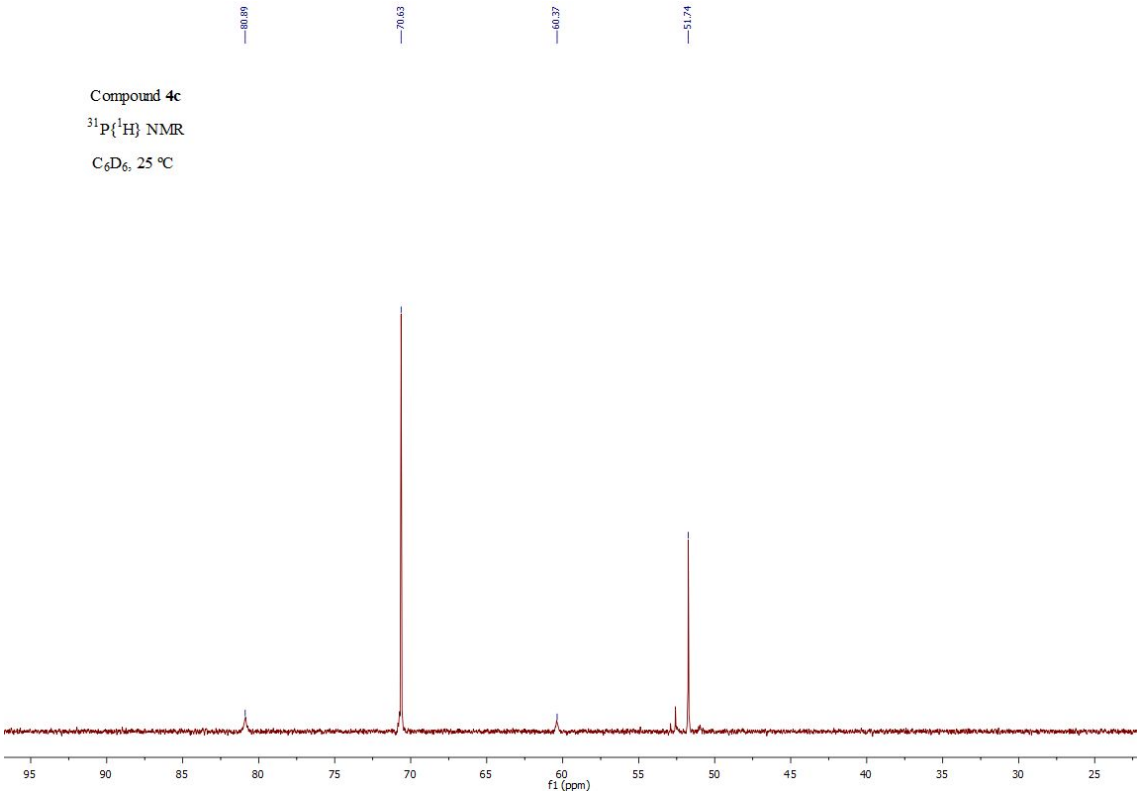

Figure S8. $^{31}P\{^{1}H\}$ NMR spectrum of compound **4c**.

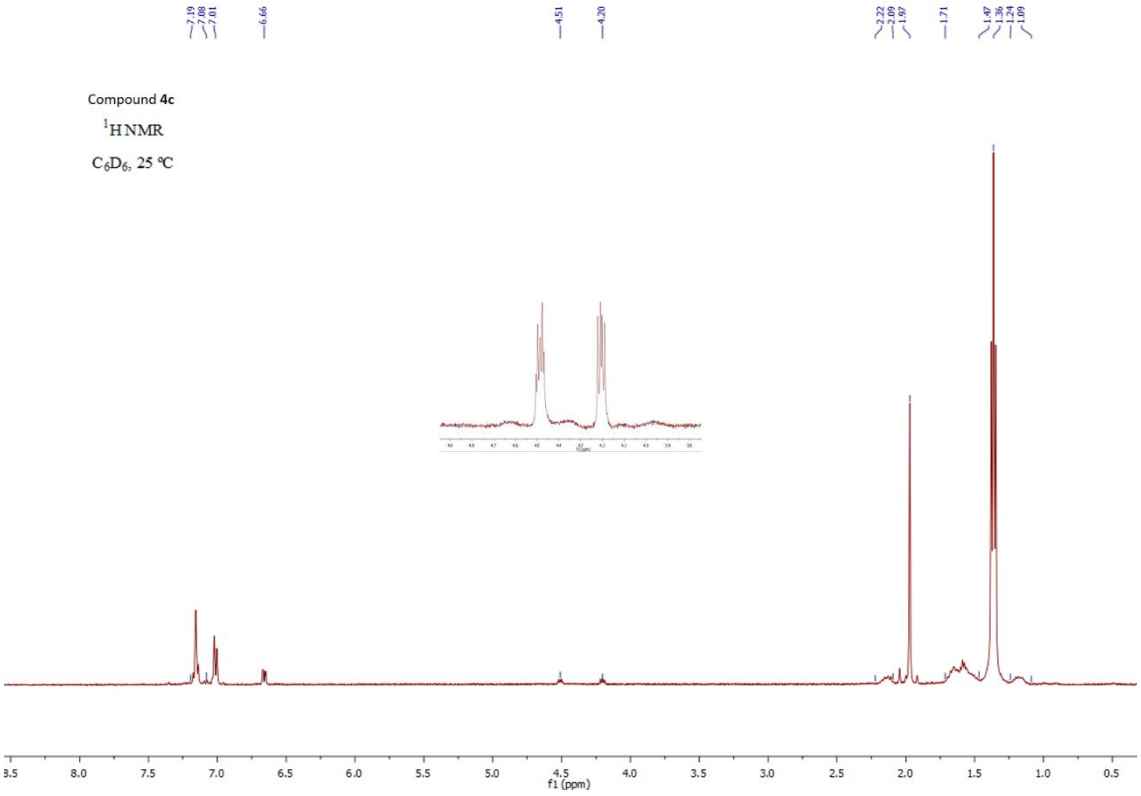

Figure S9. ^{1}H NMR spectrum of compound **4c**.

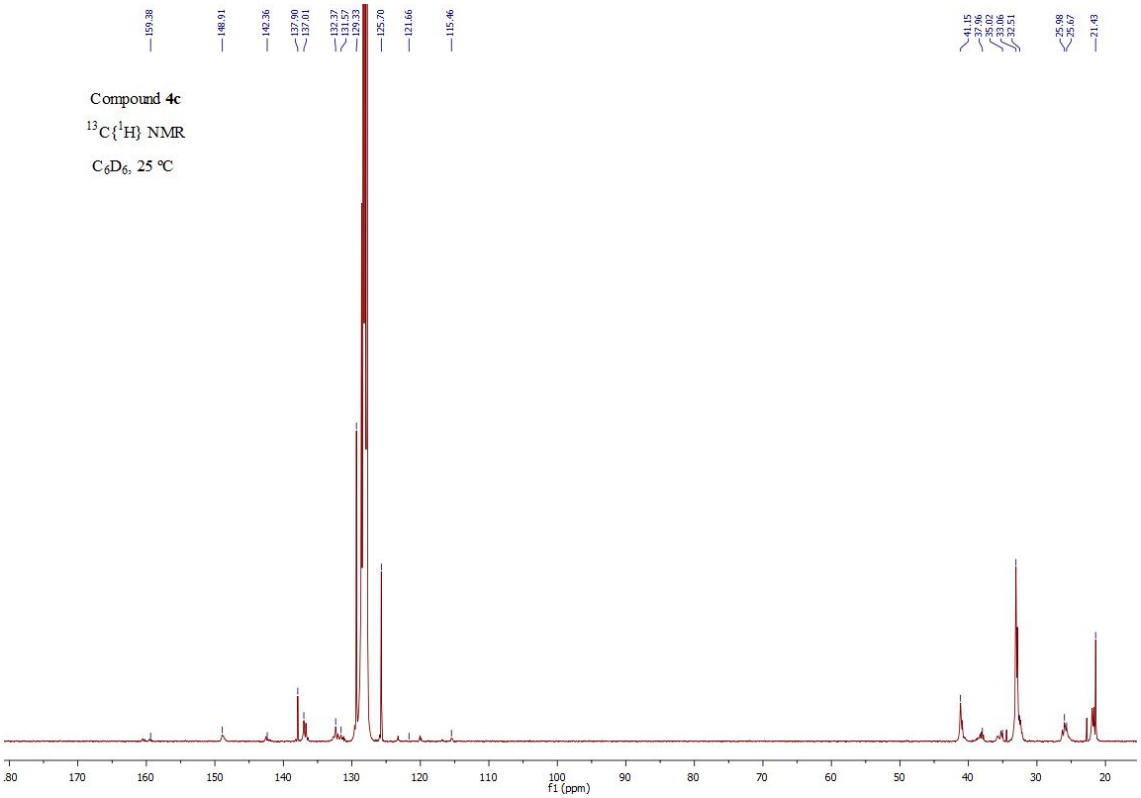

Figure S10. $^{13}C\{^{1}H\}$ NMR spectrum of compound **4c**.

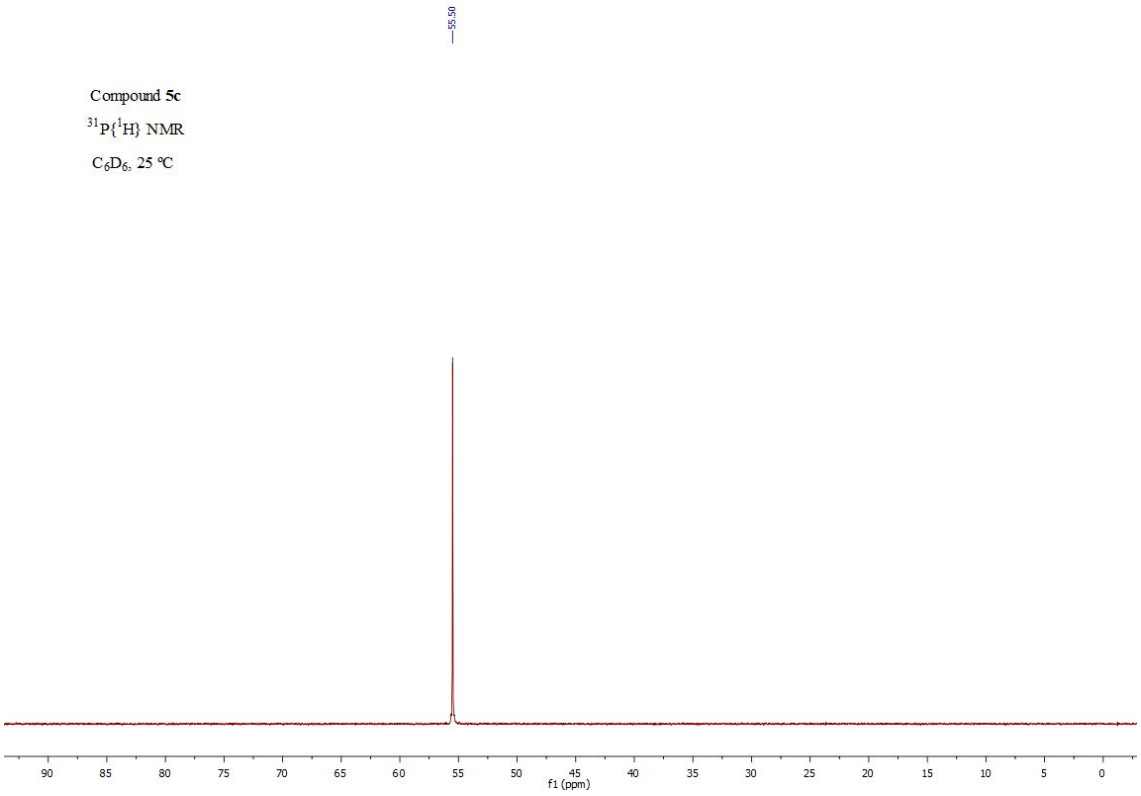

Figure S11. $^{31}P\{^{1}H\}$ NMR spectrum of compound **5c**.

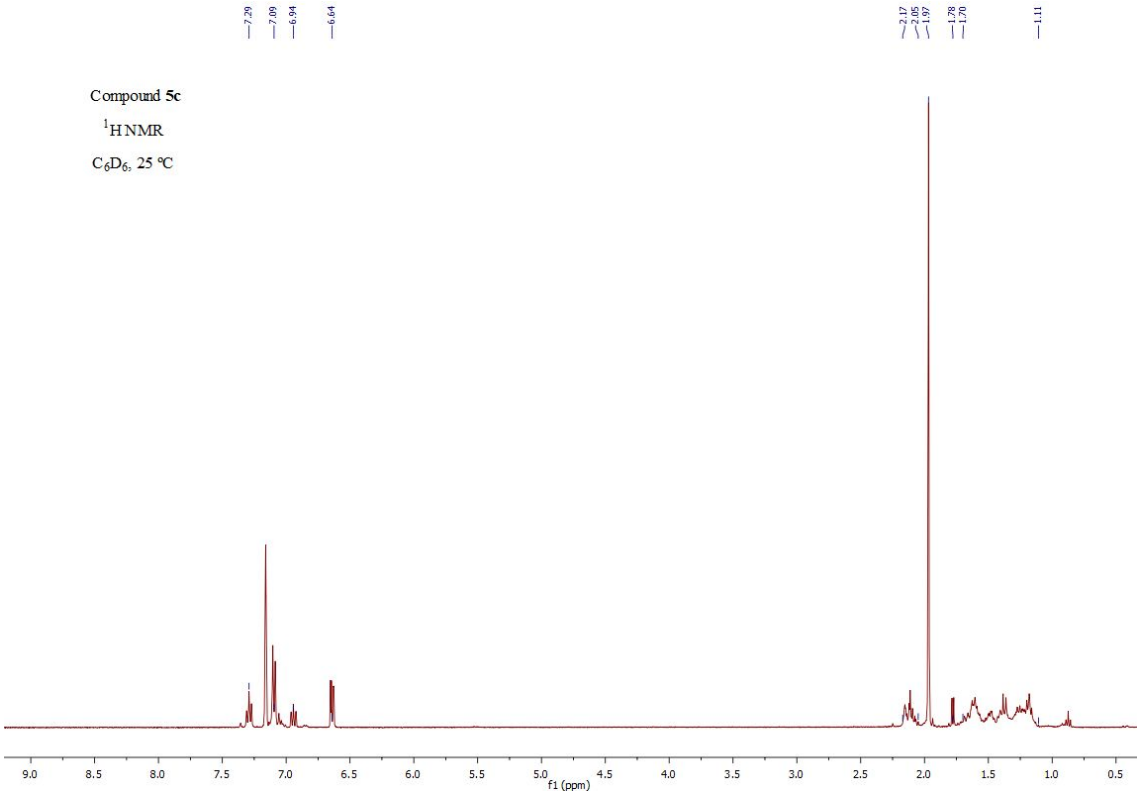

Figure S12. ^{1}H NMR spectrum of compound **5c**.

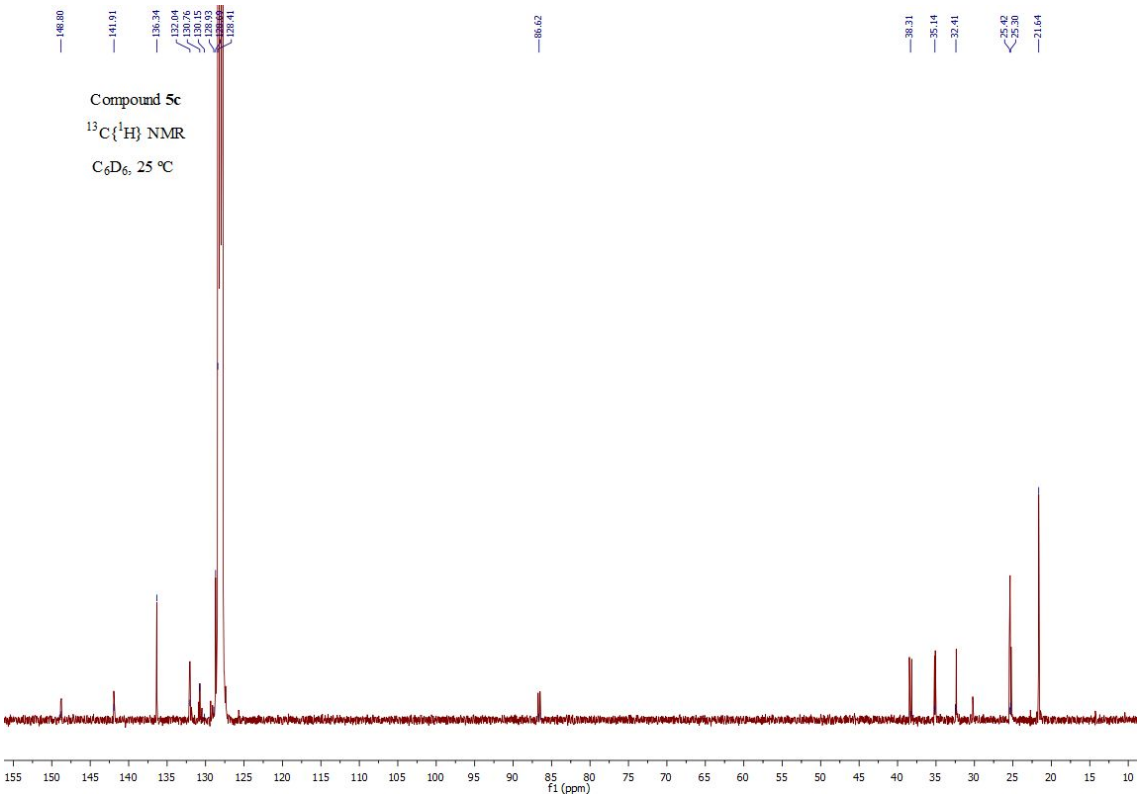

Figure S13. $^{13}C\{^{1}H\}$ NMR spectrum of compound **5c**.

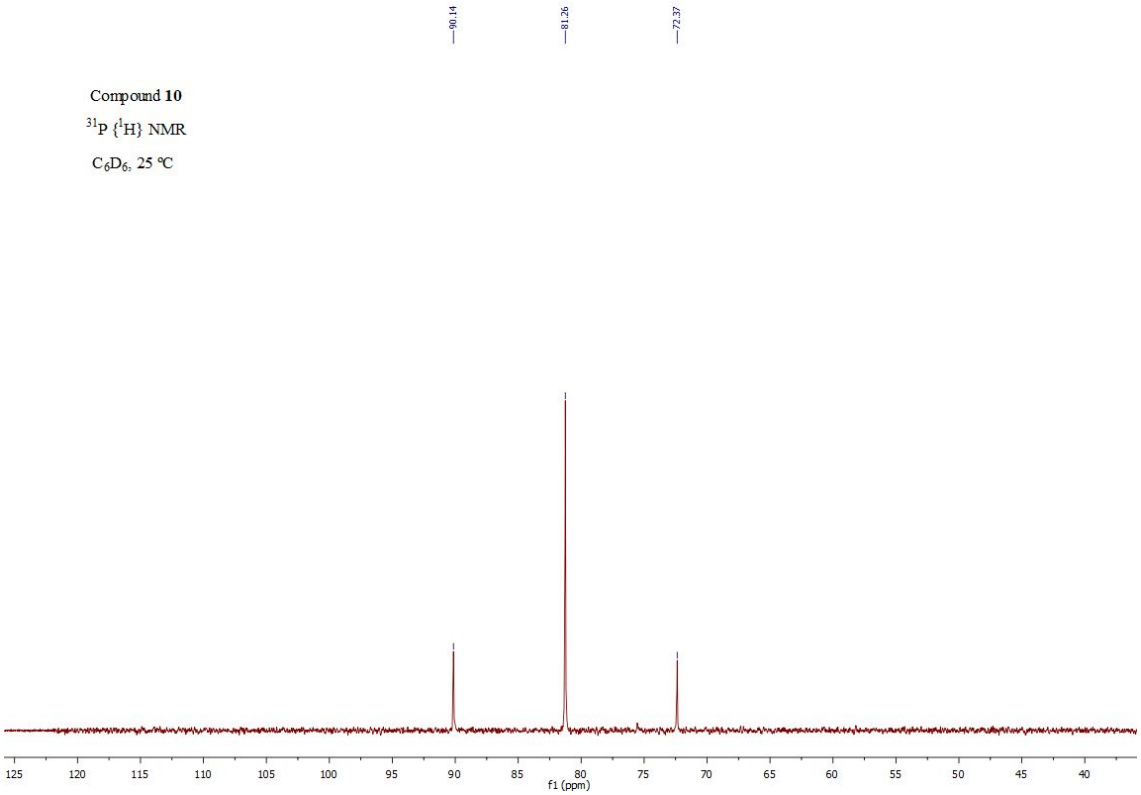

Figure S14. $^{31}P\{^{1}H\}$ NMR spectrum of compound **10**.

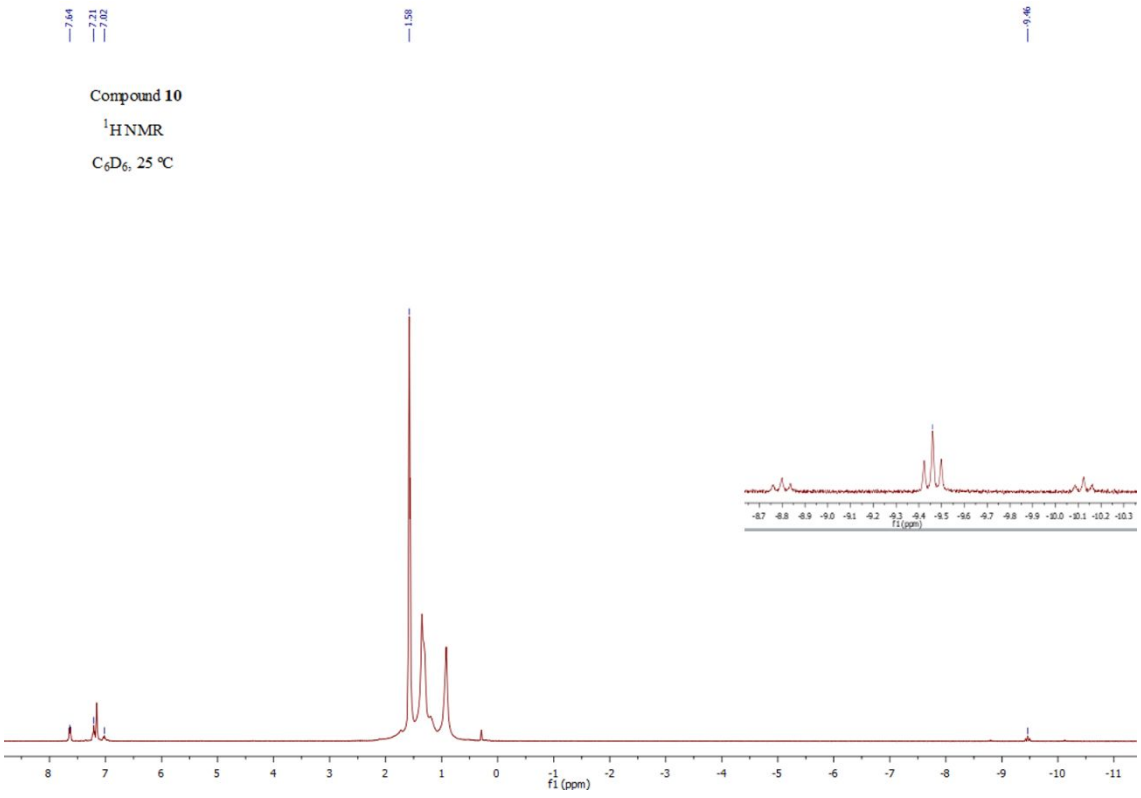

Figure S15. ^{1}H NMR spectrum of compound **10**.

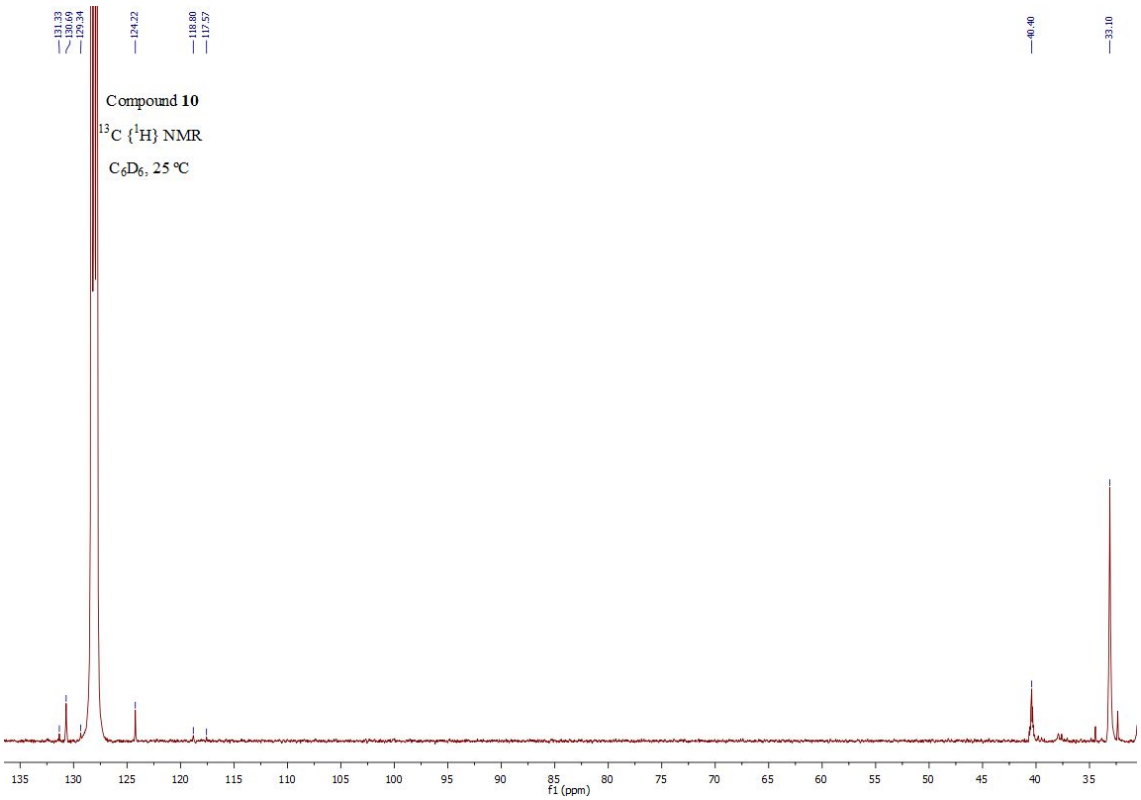

Figure S16. ^{13}C{^{1}H} NMR spectrum of compound **10**.

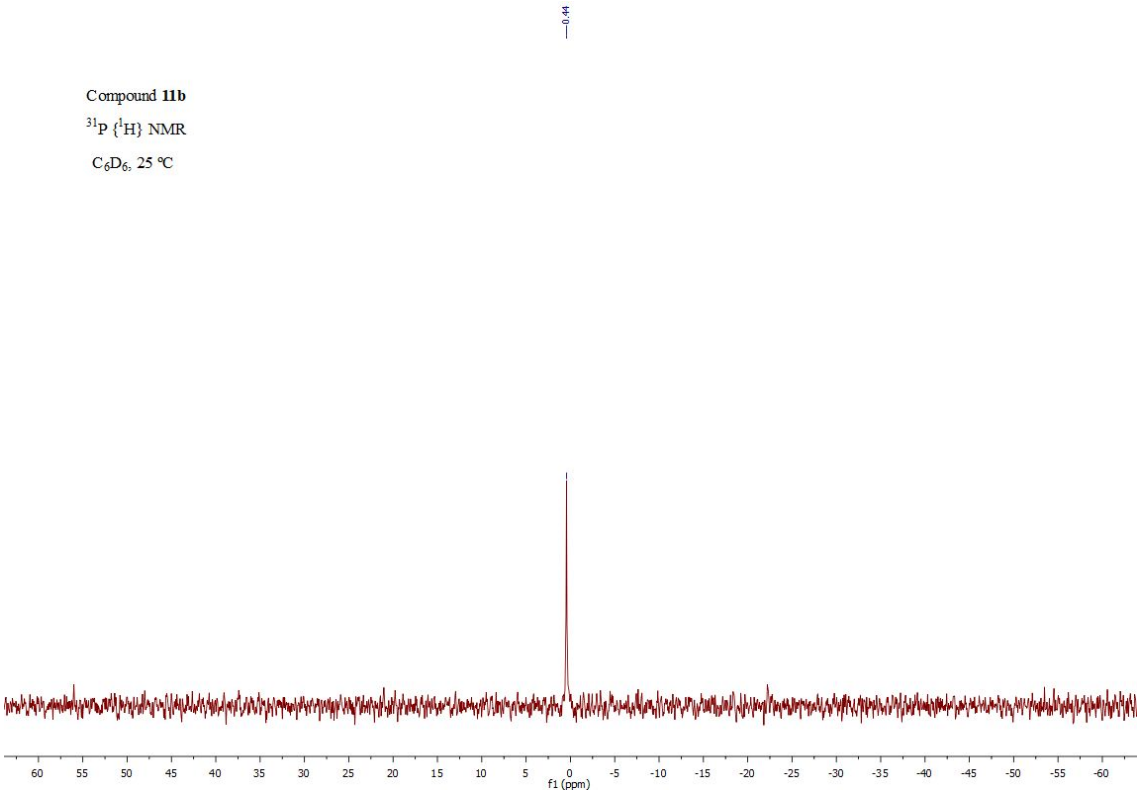

Figure S17. $^{31}P\{^{1}H\}$ NMR spectrum of compound **11b**.

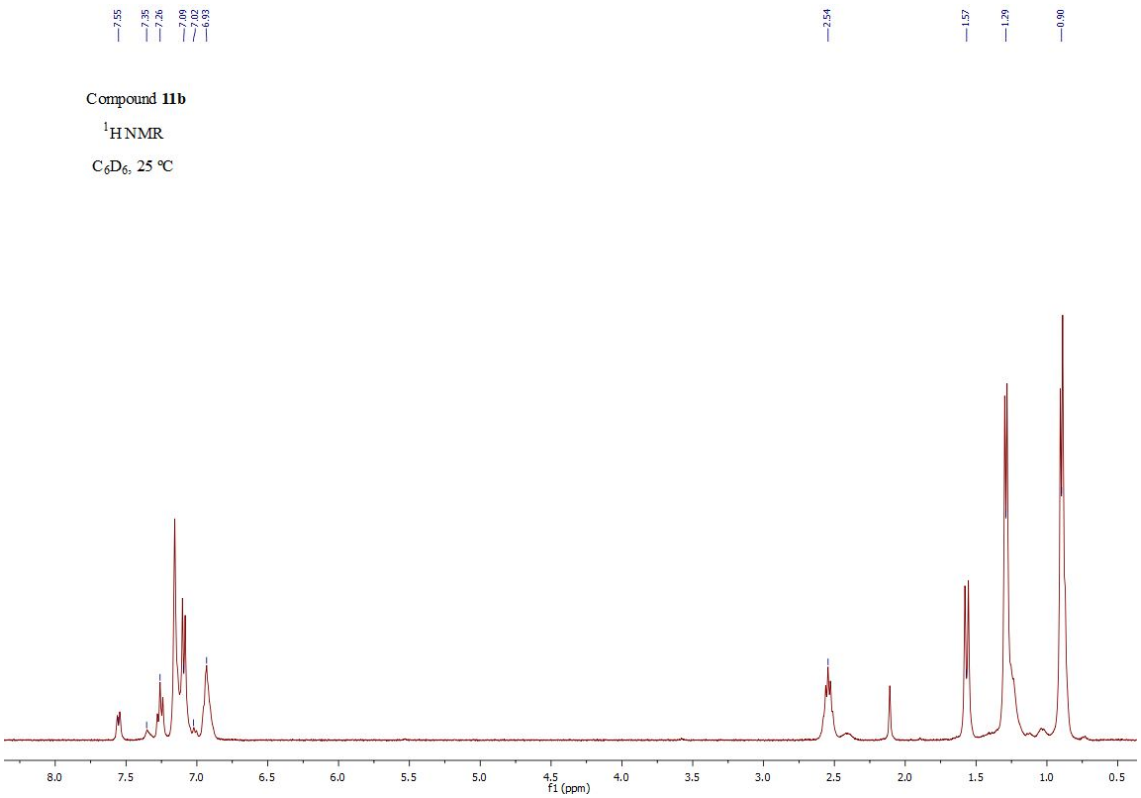

Figure S18. ^{1}H NMR spectrum of compound **11b**.

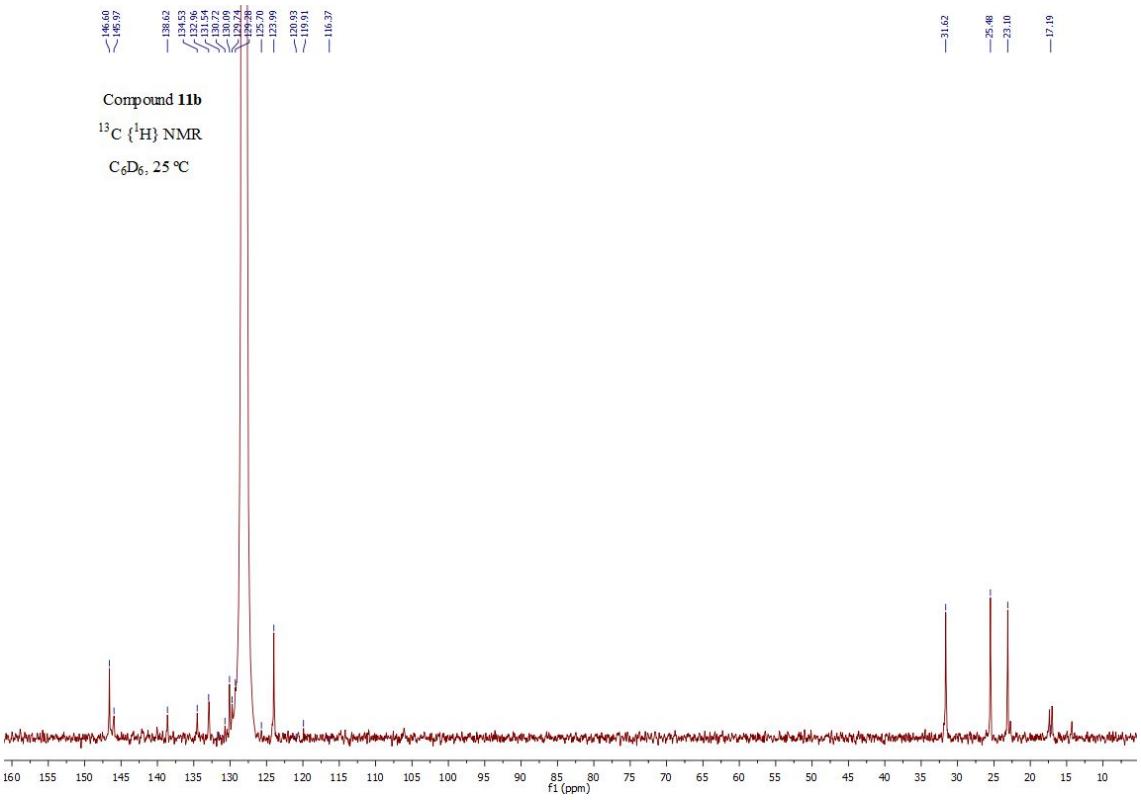

Figure S19. $^{13}C\{^{1}H\}$ NMR spectrum of compound **11b**.

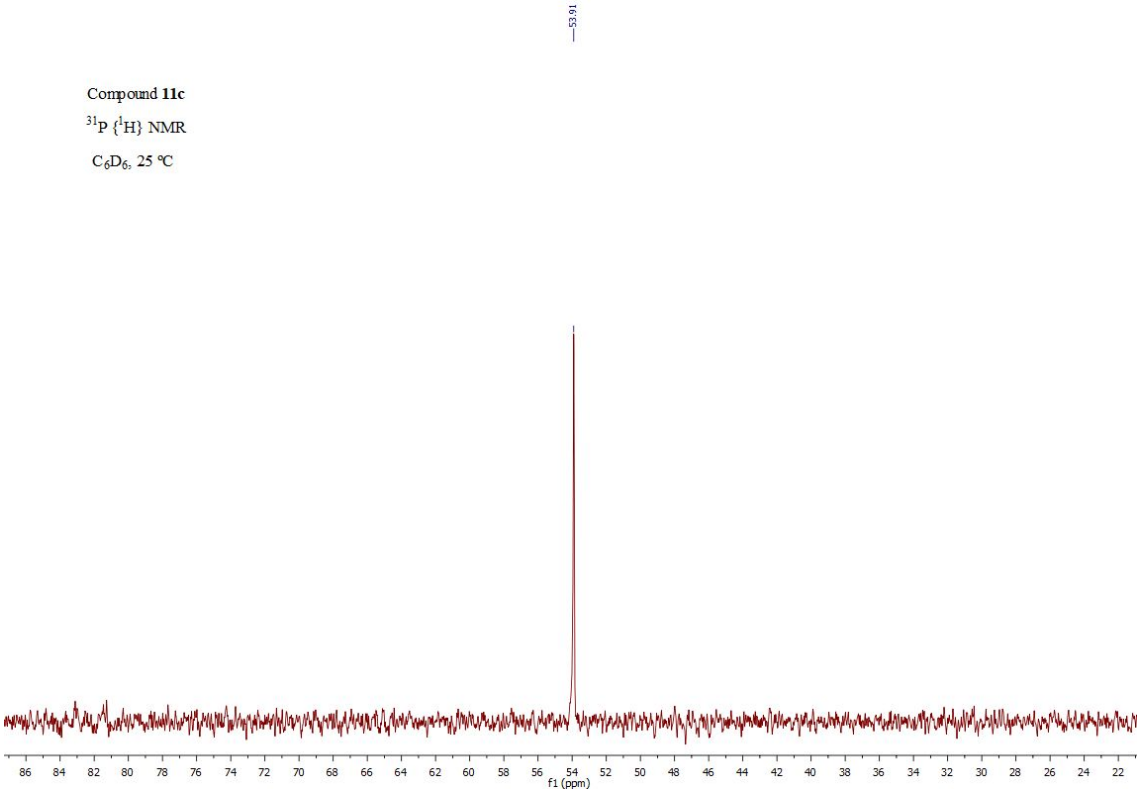

Figure S20. $^{31}P\{^{1}H\}$ NMR spectrum of compound **11c**.

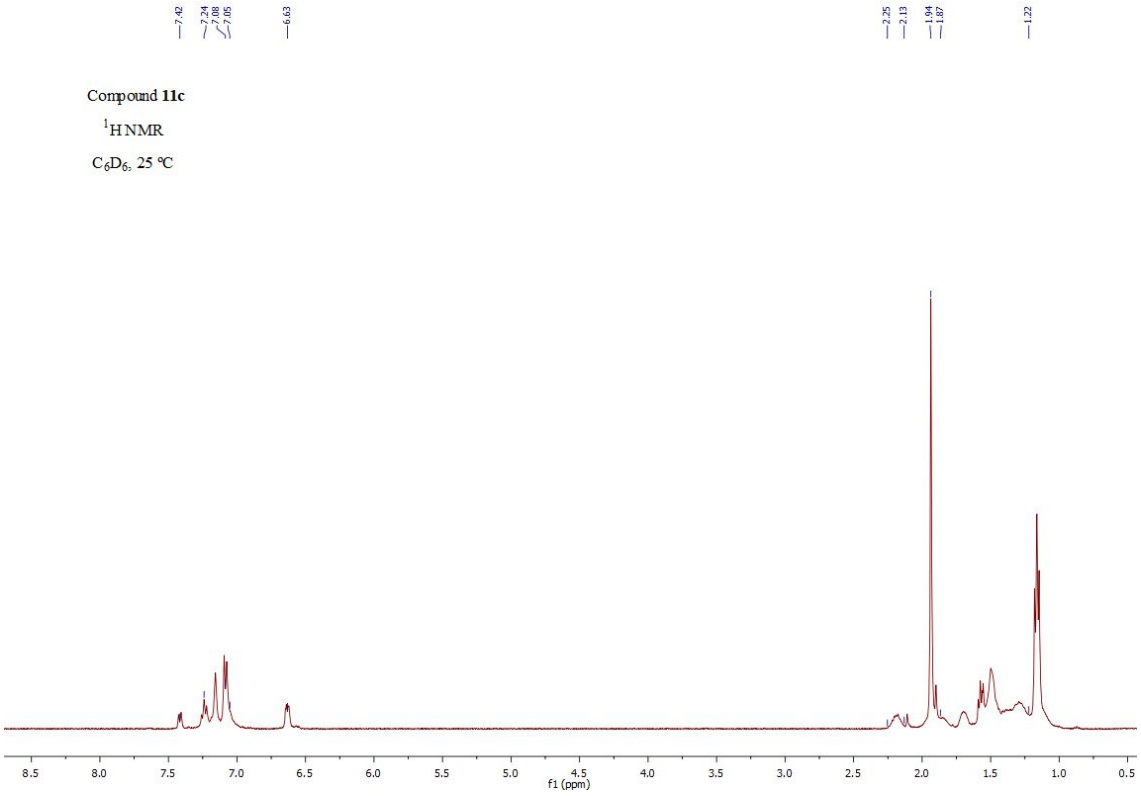

Figure S21. ^{1}H NMR spectrum of compound **11c**.

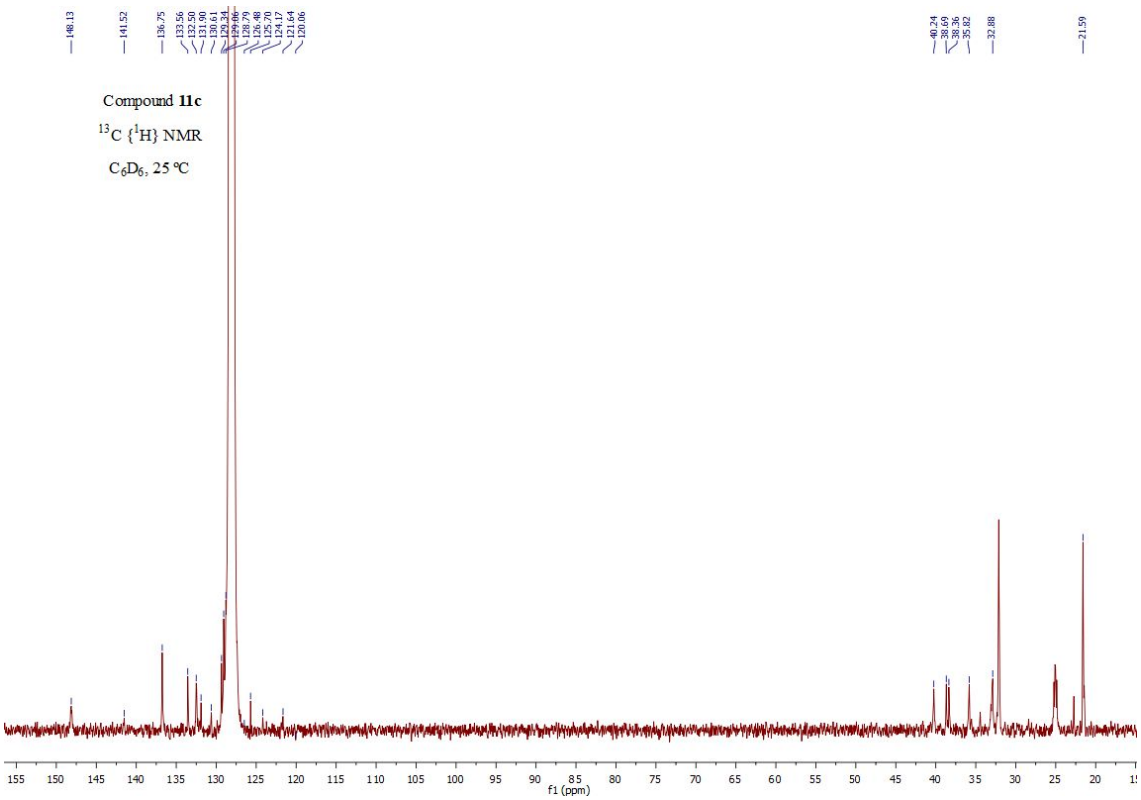

Figure S22. ^{13}C{^{1}H} NMR spectrum of compound **11c**.

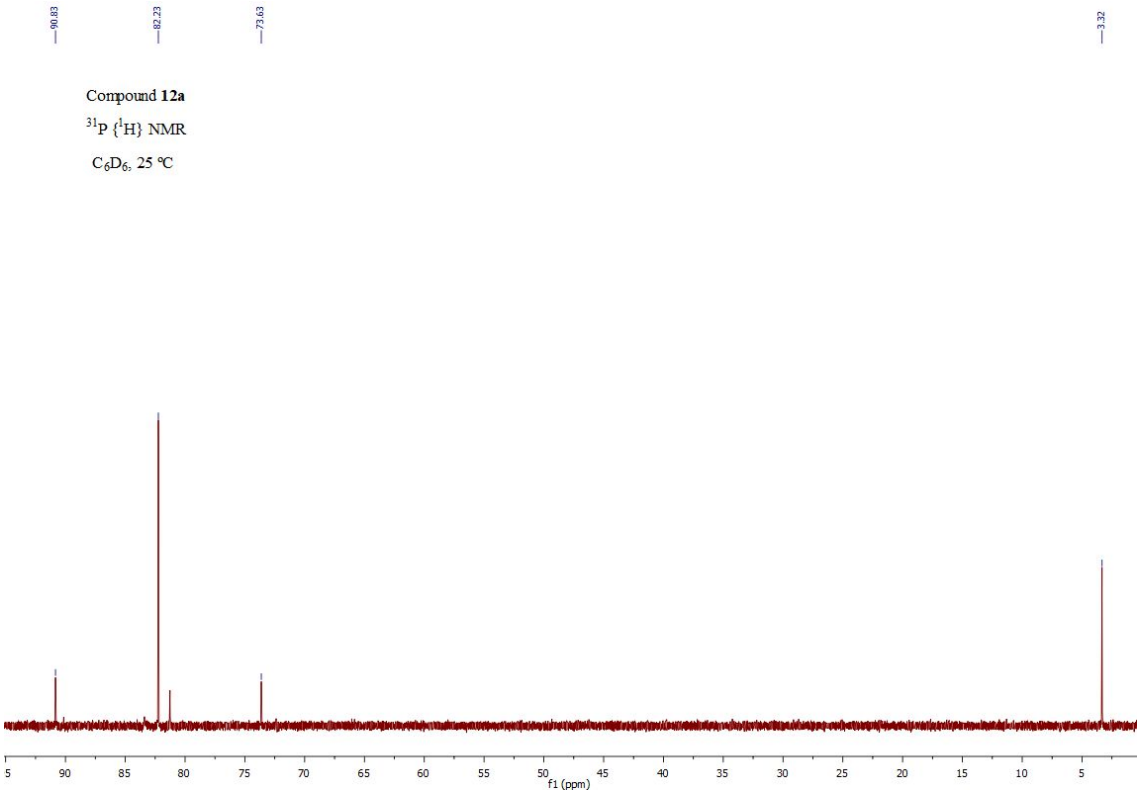

Figure S23. $^{31}P\{^{1}H\}$ NMR spectrum of compound **12a**.

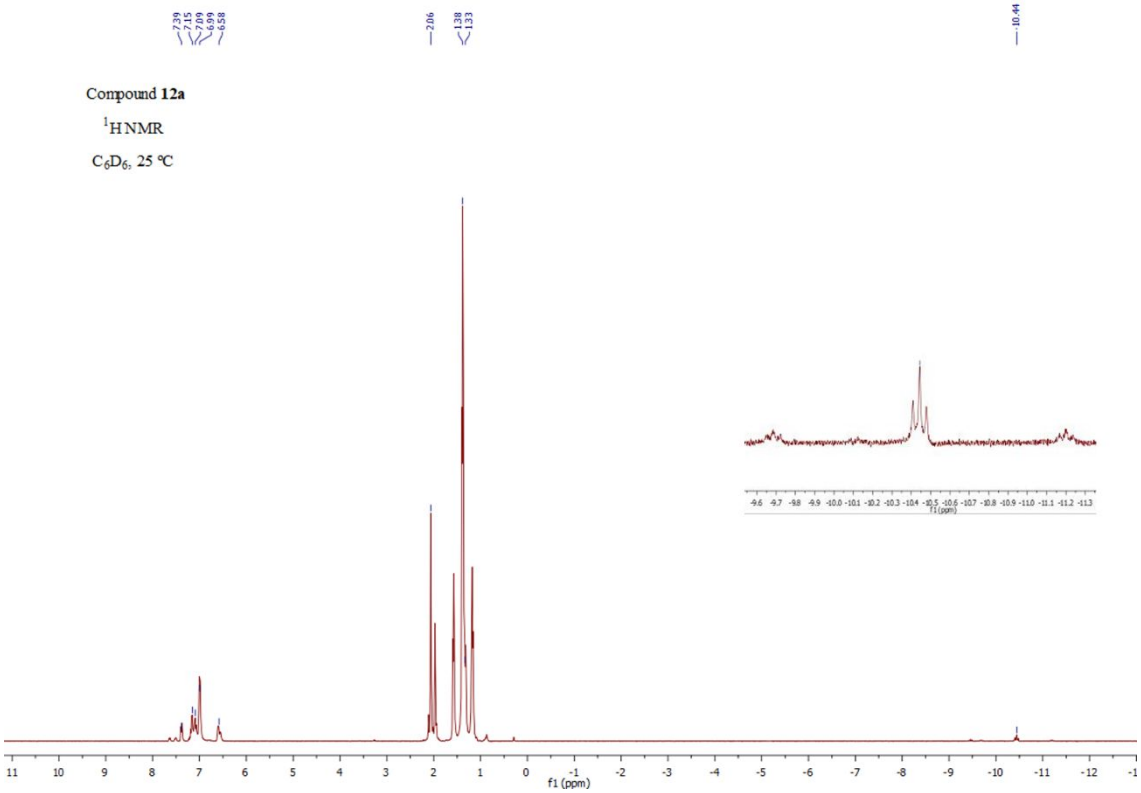

Figure S24. ^{1}H NMR spectrum of compound **12a**.

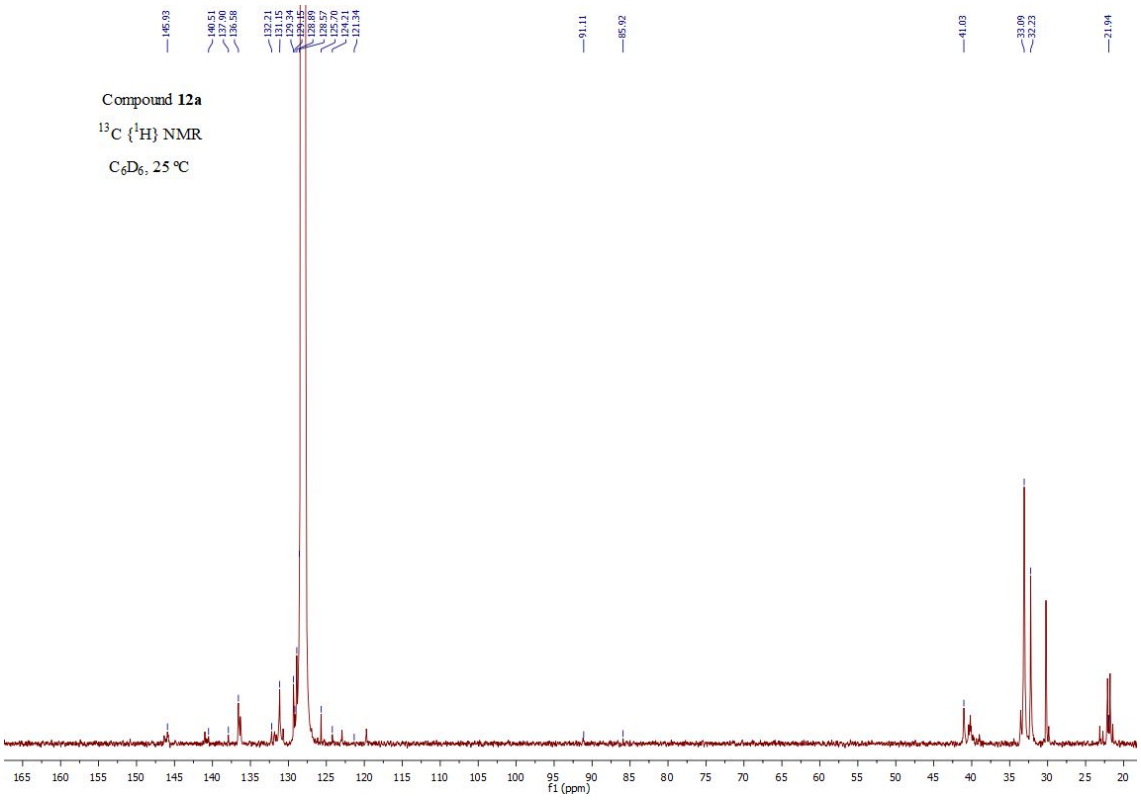

Figure S25. $^{13}C\{^{1}H\}$ NMR spectrum of compound **12a**.

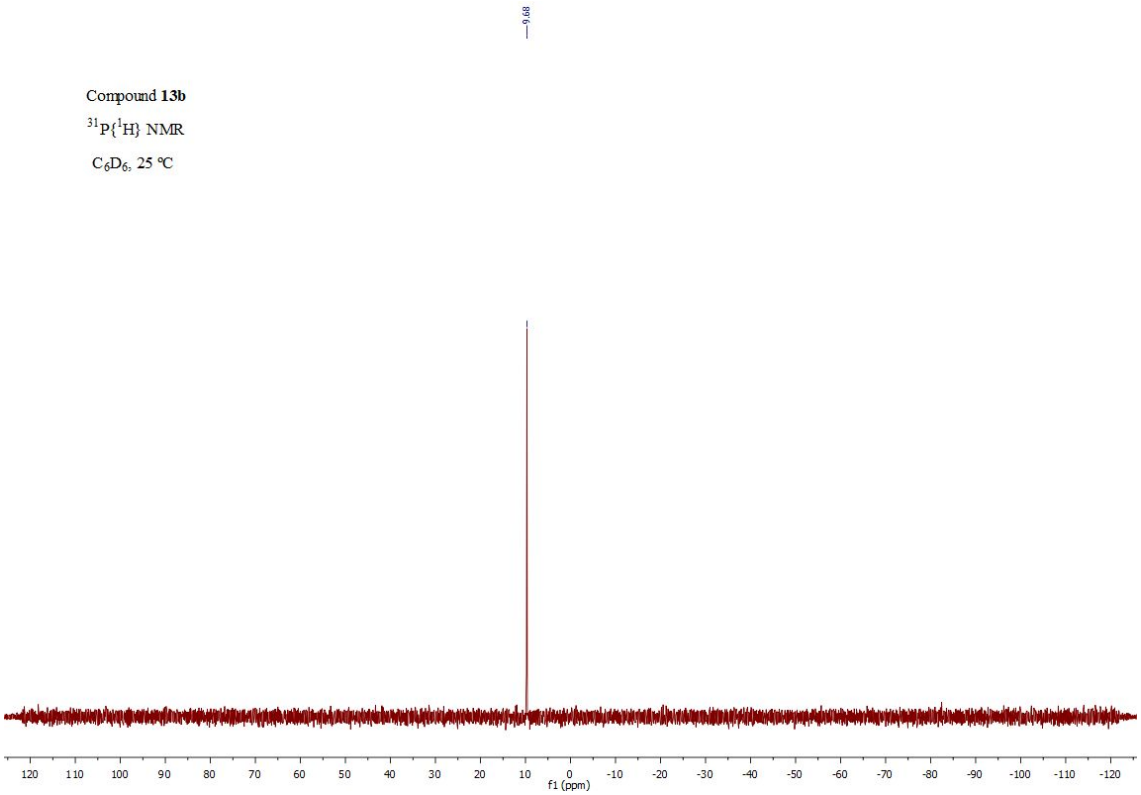

Figure S26. $^{31}P\{^{1}H\}$ NMR spectrum of compound **13b**.

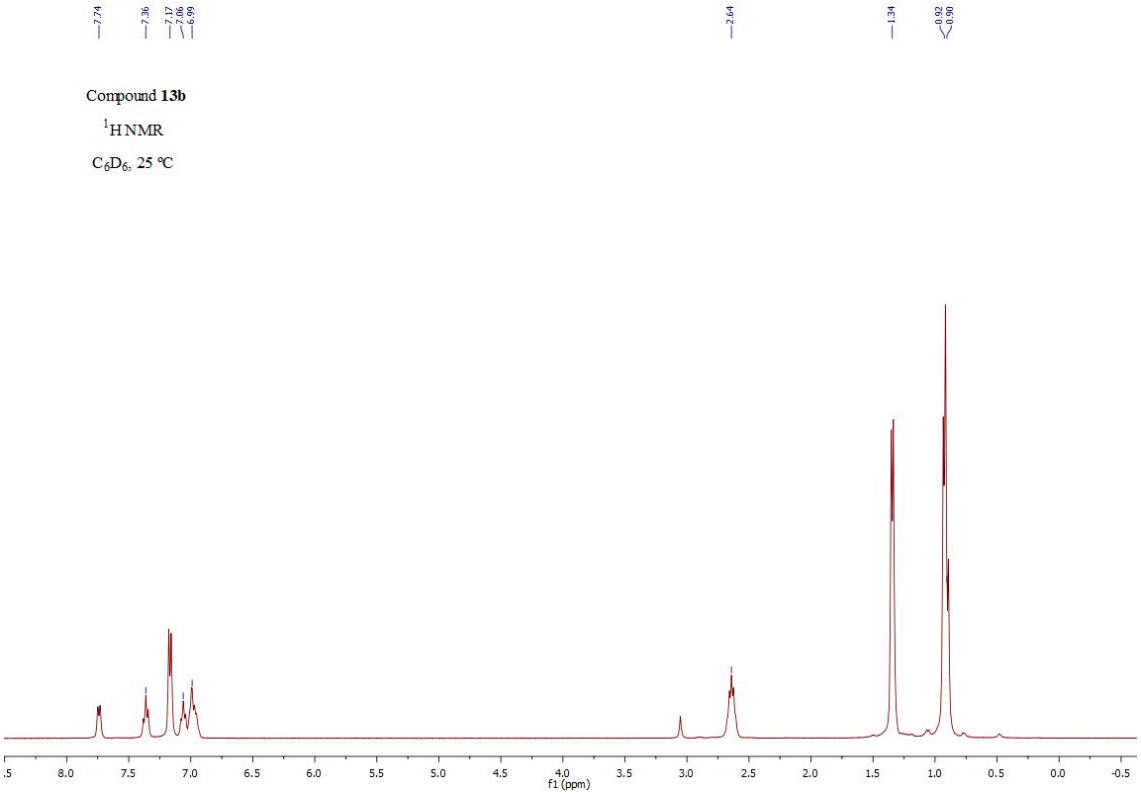

Figure S27. ^{1}H NMR spectrum of compound **13b**.

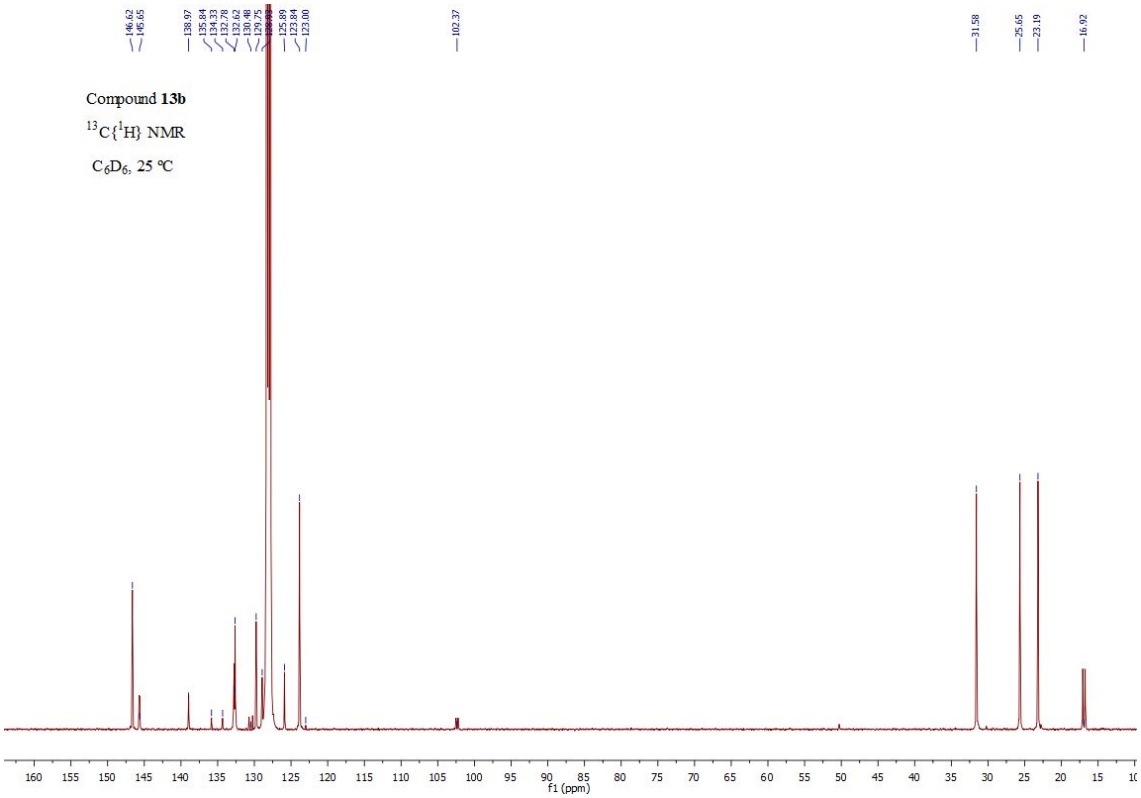

Figure S28. ^{13}C{^{1}H} NMR spectrum of compound **13b**.

4. References

[1] Sheldrick GM. SADABS, Program for Empirical Absorption Correction of Area Detector Data. Göttingen: University of Göttingen; 1996.
[2] G. M. Sheldrick, SHELXTL, version 6.14. Program for solution and refinement of crystal structures, Universität Göttingen, Germany, 2000.
[3] Spek A. L., Acta Crystallogr. C71, 2015, p. 9.